Journal of Engineering Science and Technology
Vol. 14, No. 5 (2019) 3046 - 3061

HEAT AND MASS TRANSFER OF CASSON NANOFLUID FLOW OVER A STRETCHING SHEET IN THE PRESENCE OF MAGNETIC FIELD WITH BROWNIAN AND THERMOPHORETIC EFFECTS

G. MAHANTA[1], M. DAS[2], S. SHAW[3], K. L. MAHANTA[1,*]

[1]Department of Mathematics, C. V. Raman College of Engineering, Mahura, Janla, Bhubaneswar-752054, India
[2]Department of Mathematics, School of Applied Sciences, KIIT University, Patia, Bhubaneswar-751024, India
[3]Department of Mathematics and Statistical Sciences, Botswana International University of Science and Technology, Private Bag 16, Palapye, Botswana
[*]Corresponding Author:mahantakamal@gmail.com

Abstract

We study heat and mass transfer on the flow of an electrically conducting, incompressible Casson nanofluid over the accelerated stretching plate in the presence of a magnetic field. We consider the nanofluid, which incorporates the flow effects of Brownian motion and thermophoresis. In addition, we take the convective boundary condition, slip parameter, Soret and Dufour effects on this paper. We use similarity transformation to convert non-linear partial differential equations into a set of non-linear ordinary differential equations. These ordinary differential equations are solved numerically using the Matlabbvp4c package. We discuss in detail and show graphically the influences of different physical parameters on velocity, temperature and concentration profiles. We observe that when the Casson parameter increases, the velocity field decreases, however, the temperature increases. Furthermore, we obtain the numerical values of the local skin friction coefficient, the local Nusselt and Sherwood numbers for various values of the parameters involved in the model and present these values in tabular form.

Keywords: Brownian motion, Casson nanofluid, Convective heat transfer, Mixed convection, Partial slip, Thermophoresis.

1. Introduction

The nanofluid particles obey the characteristics of convective heat transfer rate and higher thermal conductivity. Therefore, many researchers use viscous incompressible fluid flow with nano-sized fluid particles. The one-step process avoids the process of drying and dispersion of nanoparticles so that the agglomeration is minimized, and then the stability increases. The stability of nanoparticle is used as surfactants. It has many applications in industries such as advanced nuclear system. Most of the fluids like water, glycerine, and oil have very poor heat transfer rate due to low thermal conductivity. Nowadays, the use of nanoparticle is enhanced due to their Brownian motion and thermophoresis properties.

Abolbashari et al. [1], Hussein et al. [2], Rashid et al. [3] studied the Casson nanofluid, chemical reaction, viscous dissipation and magnetic field over the stretching surface. Ramzan and Bilal [4] examined 3D nanofluid flow in the presence of chemical reaction along with a magnetic field. Malvandi et al. [5] discussed the laminar flow of water nanofluid and convective heat transfer with a magnetic field inside a circular microchannel. Sreedevi et al. [6] examined the flow of heat transfer through a concentric vertical annulus. Sheikholeslami et al. [7] investigated the forced convective heat transfer of nanofluid flow in the presence of a magnetic field in between the two horizontal concentric cylinders. Mahanta and Shaw [8] also explained the Casson fluid flow in a stretching sheet with the convective boundary condition.

Rahimi-Gorji et al. [9] constructed a realistic model of human airways and studied CFD simulation of airflow behaviour and particle transport and deposition in different breathing conditions. Rahimi-Gorji et al. [10] investigated unsteady squeezing nanofluid simulation and its effect on important heat transfer parameters in the presence of a magnetic field. Rahimi-Gorji et al. [11] explored particle deposition and airflow structure of human tracheobronchial airways through a realistic model.

The zero-velocity of the viscous fluid relative to its solid boundary is known as a no-slip condition. The velocity slip and temperature jump of standard Navier's strokes and energy equations can be considered as the slip flow within the range of $0.01 < k_n < 0$. The Knudsen number ($k_n = 0$) for slip condition) the dimensionless quantity is the ratio of the molecular mean free path length to the physical length scale.

The combined use of no-slip condition, viscous-dissipation, heat transfer over a non-Newtonian fluid and Joules law of heating has been investigated by Jafari and Freidoonimehr [12], Wang [13], Sahoo [14]. The applications of Magnetohydrodynamics (MHD) flow in the industry is very important nowadays. Generally, it is used for paper production, magnetic material processing, glass manufacturing and power generation. Salem and Fathy [15] studied the properties of MHD heat and mass transfer with porous media in the presence of thermal radiation near the stagnation point towards the stretching sheet. Fang and Zhang [16] analysed analytically over a shrinking sheet, which the MHD viscous flow in a closed-form solution was analysed analytically over a shrinking sheet by

Das et al. [17] considered the Newtonian heating effect on unsteady MHDCasson fluid flow over a flat plate. They numerically and experimentally

investigated the convective boundary condition in porous media. This type of fluid flow has many applications in geothermal energy extraction industries, petroleum-processing industries. Makinde and Aziz [18], Aziz [19], Hayat et al. [20] studied the convective boundary condition, Casson nanofluid flow and stagnation point over a permeable stretching sheet in the presence of the magnetic field. Shaw et al. [21] explained their view for homogenous-heterogeneous reactions over the permeable stretching or shrinking sheet by using the micropolar fluid flow on the surface.

Shaw and Sibanda [22] examined the thermal instability in a non-Darcy porous medium using convective boundary condition at the surface. Rahimi-Gorji et al. [23] formulated a model of the air conditions effects on the power and fuel consumption of the SI engine using neural networks and regression. Further Biglarian et al. [24] studied various H_2O based nanofluids with the unsteady condition and an external magnetic field on permeable channel heat transfer.

The movement of different fluid particles is different due to the force of temperature gradient, which is called thermophoresis. The molecular effect of the fluid particles is called stochastic Brownian motion force. Michaelides [25] described the Brownian motion and thermophorsis of nanoparticles effect.

Anbuchzhian et al. [26] examined the boundary layer flow in the presence of thermal stratification due to solar energy. Furthermore, Derjaguin and Yalamov [27], Parola and Piazza [28], Hadad et al. [29] and Falana et al. [30] did a lot of work on thermophoresis and Brownian motion.

The plastic films and artificial fibres are the two important applications of the non-Newtonian fluid flow and heat transfer. It is more attractive for engineers in the last few decades. The Casson fluid flow is one of the non-Newtonian fluids, which exhibit the properties of the yield stress. When the applied yield stress is more than shear stress, then it behaves as solid. When applied yield stress is less than shear stress, then it starts to move.

In this work, we studied the thermodynamics of Casson nanofluid, velocity slip, magnetic field, convective boundary condition and thermal expansion. In addition, we discussed the effects of various flow parameters of the model governing fluid motion, heat and mass transfer characteristics with the help of figures and tables.

2. Mathematical Formulation

Consider the steady, laminar, and electrically conducting incompressible Casson nanofluid flow over-stretching plates. Furthermore, introduce the magnetic field in the governing system and convective boundary condition on the surface**.**

The surface temperature and the ambient temperature are considered a T_W and T_∞ respectively C_W and C_∞ are the concentration of nanofluid at the wall and the ambient concentration, respectively. B_0 is the magnetic field strength, which is applied normal to the direction of the fluid flow.

The induced magnetic field is negligible due to the very small magnetic Reynolds number. The domain of flow of the fluid is considered as $y > 0$. The sheet is fixed at the origin and stretched along the x-axis, which linearly related with the x-axis as $u_w\ (x) = ax$ with a constant influence of the Brownian motion and thermophoretic effects have been considered in the demonstration (Fig. 1).

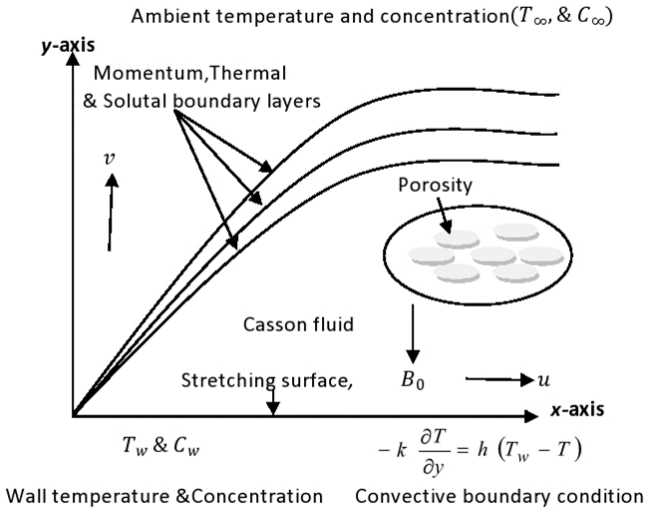

Fig. 1. Physical configuration of nanofluid flow and geometrical coordinates.

The equation of state for an isotropic and an incompressible Casson fluid flow are considered as follows:

$$\tau_{ij}=\begin{cases}2\left(\mu_B+p_y/\sqrt{2\pi}\right)e_{ij}\ , \pi>\pi_c\\ 2\left(\mu_B+p_y/\sqrt{2\pi}\right)e_{ij},\quad \pi<\pi_c.\end{cases} \tag{1}$$

Here $\pi = e_{ij}e_{ij}$ and e_{ij} is the deformation rate of $(i, j)th$ components, π is the product deformation rate by itself, π_c is the critical value based on non-Newtonian form, μ_B is the dynamic viscosity based on non-Newtonian fluid and p_y is the yield stress of the fluid. The basic two-dimensional equations governing the conservations of mass, momentum, and energy and nano-particle flow of the Casson fluid by means of the above assumptions with Boussinesq approximation for incompressible fluid are given by:

$$\frac{\partial u}{\partial x}+\frac{\partial v}{\partial y}=0, \tag{2}$$

$$u\frac{\partial u}{\partial x}+v\frac{\partial u}{\partial y}=\nu\left(1+\frac{1}{\beta}\right)\frac{\partial^2 u}{\partial y^2}-\frac{\sigma B^2}{\rho f}u+g\left[\beta_T(T-T_\infty)+\beta_C(C-C_\infty)\right] \tag{3}$$

$$u\frac{\partial T}{\partial x}+v\frac{\partial T}{\partial y}=\alpha\left(\frac{\partial^2 T}{\partial x^2}+\frac{\partial^2 T}{\partial y^2}\right)+\tau\left[D_B\left(\frac{\partial C}{\partial x}\frac{\partial T}{\partial x}+\frac{\partial C}{\partial y}\frac{\partial T}{\partial y}\right)+\frac{D_T}{T_\infty}\left\{\left(\frac{\partial T}{\partial x}\right)^2+\left(\frac{\partial T}{\partial y}\right)^2+\frac{\nu}{C_p}\left(1+\frac{1}{\beta}\right)\left(\frac{\partial u}{\partial y}\right)^2\right\}\right] \tag{4}$$

$$u\frac{\partial C}{\partial x}+v\frac{\partial C}{\partial y}=D_B\left(\frac{\partial^2 C}{\partial x^2}+\frac{\partial^2 C}{\partial y^2}\right)+\frac{D_T}{T_\infty}\left(\frac{\partial^2 T}{\partial x^2}+\frac{\partial^2 T}{\partial y^2}\right). \tag{5}$$

where the velocity components u and v are considered in the x and y- directions respectively, ν is the kinematic viscosity, ρ is the fluid density, $\beta=\mu_B\sqrt{2\pi_c}/p_y$ is the Casson fluid parameter, α represents the thermal diffusivity, C_p is the specific heat at

constant temperature, $\tau = (\rho c)_p / (\rho c)_f$ is the ratio of the heat capacity of the nanofluids of the given material to the base fluid; *C* and *T* are considered as the concentration; and the temperature of the fluid, D_B and D_T are considered as the Brownian; and thermophoretics diffusion coefficient respectively. The corresponding boundary conditions are as follows:

$$u = u_w(x) + \gamma_0 \frac{\partial u}{\partial y}, v = 0, -k \frac{\partial T}{\partial y} = h(T_w - T), C = C_w \text{ at } y = 0 \tag{6}$$

$$u \to 0, v \to 0, T \to T_\infty, C \to C_\infty \text{ as } y \to \infty. \tag{7}$$

y_o is the length of the slip parameter at a relative constant of the velocity, *k* is the thermal conductivity and *h* is a convective heat transfer coefficient. Now let us use the following similarity transformation and dimensions variables in the governing Eqs. (2) to (4).

$$u = u_w f'(\eta), \; v = -\sqrt{\frac{\nu u_w}{x}} f(\eta), \theta(\eta) = \frac{T - T_\infty}{T_W - T_\infty}, \; \varphi(\eta) = \frac{C - C_\infty}{C_W - C_\infty}, \; \eta = \sqrt{\frac{u_W}{\nu x}}\, y \tag{8}$$

where, f, θ and φ are the field of velocity, temperature and concentration of the fluid, respectively, and η is a scale boundary-layer coordinate. Equations (2) to (4) become:

$$\left(1 + \frac{1}{\beta}\right) f'''(\eta) + ff'' - (f')^2 + Gr\,\theta(\eta) + Gc\,\varphi(\eta) - M\, f'(\eta) = 0, \tag{9}$$

$$\theta'' + \Pr f(\eta)\theta'(\eta) + Nb\,\theta'(\eta)\varphi'(\eta) + Nt(\theta'(\eta))^2 + \left(1 + \frac{1}{\beta}\right) \Pr Ec\, f''^2 = 0, \tag{10}$$

$$\varphi'' + Le\, f(\eta)\varphi'(\eta) + \frac{Nt}{Nb} + \theta''(\eta) = 0. \tag{11}$$

where $\Pr = \frac{\nu}{\alpha}$, $Nb = \frac{\tau D_B (C_w - C_\infty)}{\alpha}$, $Nt = \frac{D_T (T_W - T_\infty)\tau}{\alpha T_\infty}$, $Le = \frac{\nu}{D_B}$, $Gr = \frac{g\beta_T (T_W - T_\infty)}{a^2 x}$, $Gc = \frac{g\beta_T (C_W - C_\infty)}{a^2 x}$.

The corresponding boundary conditions Eqs. (6) and (7) will be reduced to:

$$f(0) = 0, \; f'(0) = 1 + \gamma f''(0), \; \theta' = -Bi(1 - \theta(0)), \; \varphi(0) = 1 \tag{12}$$

$$f'(\infty) = 0, \; \theta(\infty) = 0, \; \varphi(\infty) = 0. \tag{13}$$

where $Bi = \frac{h}{k}\left(\sqrt{\frac{\nu}{a}}\right)$

The skin friction coefficient, the Local Nusselt and Sherwood number are defined as:

$$C_f = \frac{\tau_w}{\rho u_w^{\,2}(x)}, Nu_x = \frac{x q_w}{k(T_w - T_\infty)}, Sh_x = \frac{x q_m}{D_B(C_w - C_\infty)} \tag{14}$$

where, q_w and q_m are the heat and mass flux at the surface. Now the reduced skin friction, Nusselt and Sherwood number are:

$$\mathrm{Re}_x^{\frac{1}{2}} C_f = \left(1+\frac{1}{\beta}\right) f''(0), Nu_r = \frac{Nu_x}{\mathrm{Re}_x^{\frac{1}{2}}} = -\theta'(0), Sh_r = \frac{Sh_x}{\mathrm{Re}_x^{\frac{1}{2}}} = -\varphi'(0) \tag{15}$$

where, $\mathrm{Re} = \frac{u_w(x)}{\nu}$ is the Reynolds number, based on stretching velocity $u_w(x)$.

3. Results and Discussion

In the preceding section, we solved the differential Eqs. (8) to (10) along with the boundary conditions Eqs. (11) and (12) using the Matlab package bvp4c.The properties of the fluid flow and its heat and mass transfer for different leading parameter values are shown in the graphs given below. Further, we have discussed the results for Casson nanofluid and compared the results with the Newtonian fluid.β = 0.5, M = 1.0, Gr = 0.6, Gc = 0.5, Nb = Nt = 0.1, Le = 2.0, Pr = 0.57, γ = 0.5 and β= 0.5are the fixed values of the parameters. In Table 1, we have made a comparative study of Sherwood number with the work of Abolbashari et al. [1] and it is found to be in excellent agreement with our results.

Table 1. Comparison of reduced Sherwood number when Nt = Nt= 0.5, Le = 5.0, Bi = 0.1, b → ∞.

Pr	Results of Abolbashari et al. [1]	Present results
1	1.5477	1.5476
2	1.5554	1.5554
3	1.5983	1.5983

The result of a thermal Grashof number on velocity field has been depicted in Fig. 2(a). By increasing the thermal Grashof number, we observe that the flow of the fluid velocity is accelerated due to enrichment in buoyancy force. Further, it observed that the velocity profile influences at its boundary layer for both Casson nanofluids and Newtonian fluid. However, we noted that the velocity of the fluid was larger for the non-Newtonian Casson fluid that the Newtonian fluid, which was a familiar result of Hayat et al. [20]**.** Figures 2(b) and 3(a) showed that the variations in the field of temperature and concentration of the different values of thermal Grashof number (Gr) decreased due to natural convection for both Newtonian as well as Casson nanofluids.

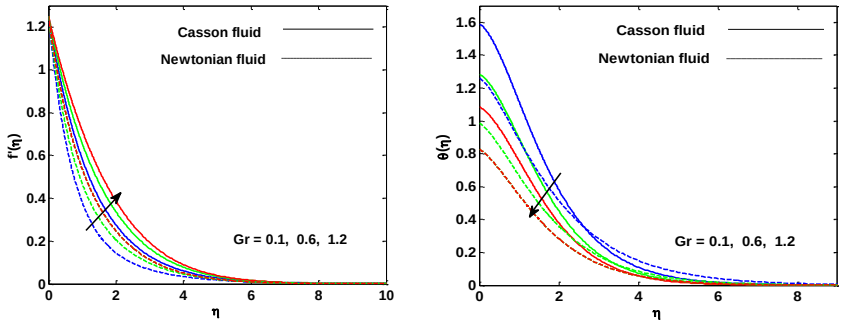

(a) Velocity profile for Gr. **(b) Temperature profile for Gr.**

Fig. 2. Velocity and temperature profiles.

Figures 3(b) put on view the outcome of Brownian motion (Nb) on the velocity profile. It is clear from these figures that the fluid velocity of Casson and Newtonian fluid flow decreases for Brownian motion. The velocity picture of the thermophoresis enhanced due to the temperature gradient. The effect on the temperature and concentration profile due to Nb and Nt are displayed in Figs. 4(a) and (b). Figure 5(a) put on view the outcome of thermophoresis (Nt). It is clear from this figure that velocity profile increases for thermophoresis parameter due the movement of nanoparticle. Figures 5(b) and 6(a) shows the effect on the temperature and concentration profiles due to Nt. The heat and mass transfer rate increases with Nb and Nt on the surface, respectively. With an increase in the Nb and as well as Nt parameters there is an enhancement of the heat throughout the system. Therefore, the distribution of nanoparticle in the flow over the stretching surface can be approved via the mechanism of Brownian motion and the cooling area can also be executed via smaller values of Nb and Nt. However, maximum concentration boundary layer thickness is gained with minimum Nb values, however, with the hike, the values of Nt the boundary layer thickness is grown. Hence, Nt assists the nanofluid particle diffusion as a result of the thermophoresis effect, which reflects a similar result of Falana et al. [30]. The concentration boundary layer thickness enhanced due to the reduction of the mass transfer rate. Moreover, the concentration boundary layer thickness not much significant due to changes in the rheology of the fluid.

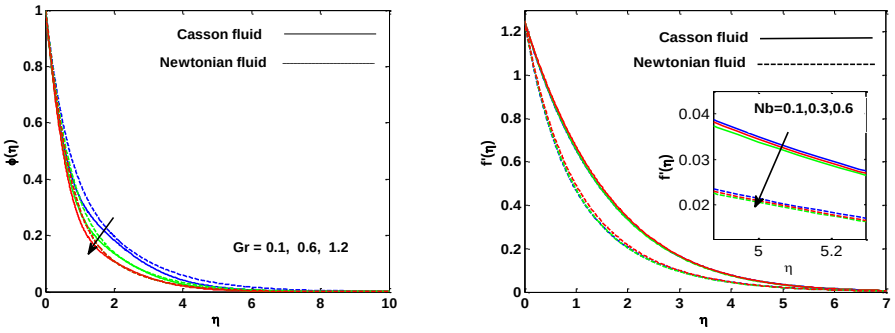

(a) Concentration profile for Gr. **(b) Velocity profile for Nb.**

Fig. 3. Concentration and velocity profiles.

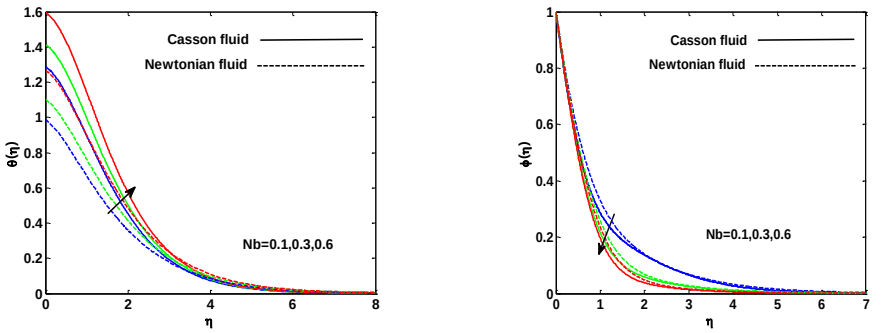

(a) Temperature profile for Nb **(b) Concentration profile for Nb**

Fig. 4. Temperature and concentration profiles.

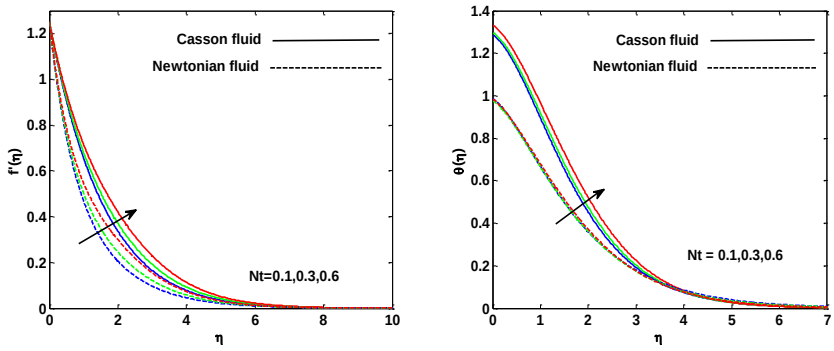

(a) Velocity profile for Nt. **(b) Temperature profile for Nt.**

Fig. 5. Velocity and temperature profiles.

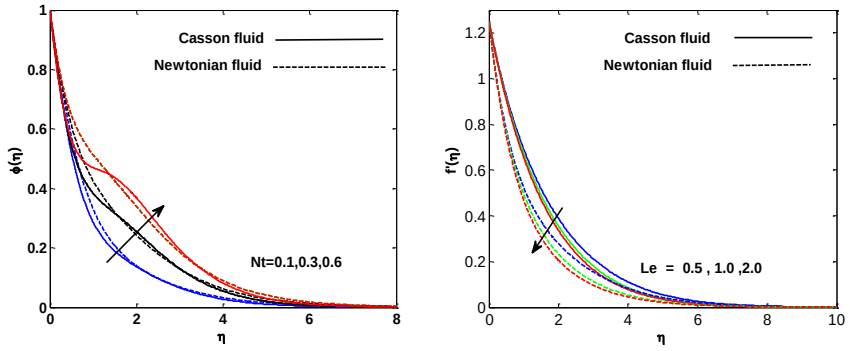

(a) Concentration profile for Nt. **(b) Velocity profile for Le.**

Fig. 6. Concentration and velocity profile.

Lewis number is used to characterize the fluid flows where there are simultaneous heat and mass transfer by convection. For the cases of Lewis number, the velocity profile decreases due to convection as shown in Fig. 6(b). The thermal boundary layer thickness increases for higher values of the Lewis number due to thermal diffusivity as shown in Figs. 7(a) and (b) shows the variations in the concentration profiles of both the fluids for Le. It is noticed that the concentration boundary layer thickness decreases as Le increases. Lewis number enhanced the mass diffusivity of the system, which reduced the boundary layer thickness of solutal concentration. Figure 8(a) represents the variation of Eckert number on the velocity profile. The velocity profiles increase with the increase in the Eckert number due to kinetic energy. For smaller Eckert number, the terms in the energy equations describing the pressure changes, and body force in energy can be neglected. Therefore, temperature and concentration profile increases with an increase in the Eckert number as it observed from Figs. 8(b) and 9(a).The Biot number influences the velocity due to convection, which is clearly shown in Fig. 9(b). The heat transfer rate increases with an increase in the Biot number. Further, it is also observed from Fig.10 (a), that the thermal boundary layer thickness increases with an increase in the Biot number.

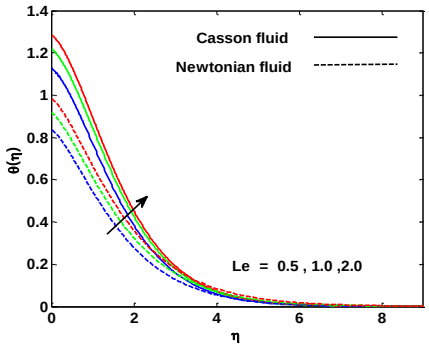

(a) Temperature profile for Le.

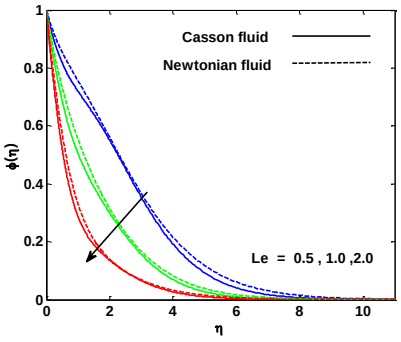

(b) Concentration profile for Le.

Fig. 7. Temperature and concentration profile.

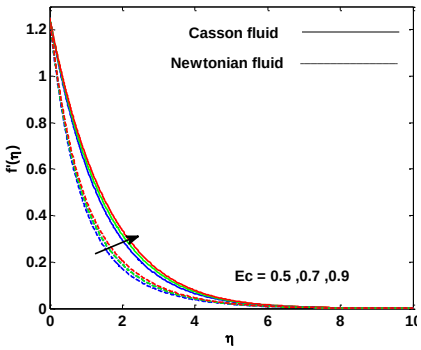

(a) Velocity profile for Ec.

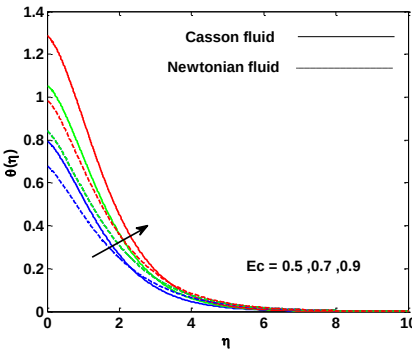

(b) Temperature profile for Ec.

Fig. 8. Velocity and temperature profiles.

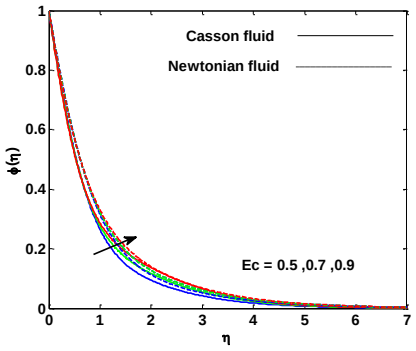

(a) Concentration profile for Ec.

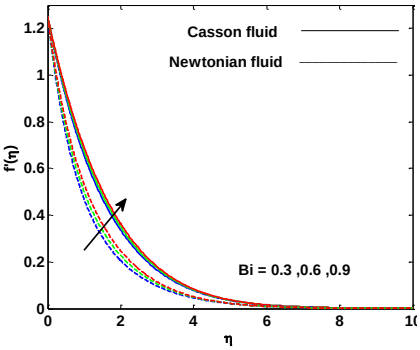

(b) Velocity profile for Bi.

Fig. 9. Concentration and velocity profiles.

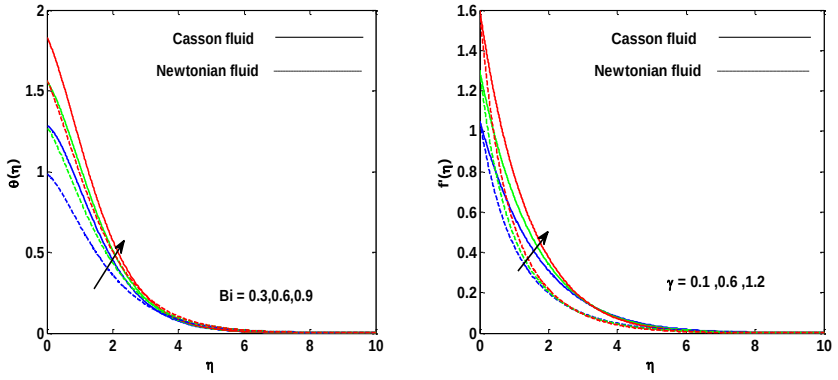

(a) Temperature profile for Bi. **(b) Velocity profile for γ.**

Fig. 10. Temperature and velocity profiles.

Since there is no slip on the walls for real fluids, it is found that with access the slip parameter, the velocity profiles increased and concentration profile decreased, for Newtonian and Casson's fluid has displayed in Figs.10(b) and 11(a).

The effect of magnetic parameter on the velocity, temperature and concentration profiles are illustrated in Figs. 11(b), 12(a) and (b).It is now well established fact that the magnetic field presents a damping effect on the velocity field by creating a drag force that opposes the fluid motion, which is known as Lorentz force and gives an additional resistance in the system and its impact on the to decrease with increase in the magnetic field for Casson nanofluid as well as Newtonian fluid.

Both temperature field as well as concentration field increase with the respective increase in the magnetic parameter.

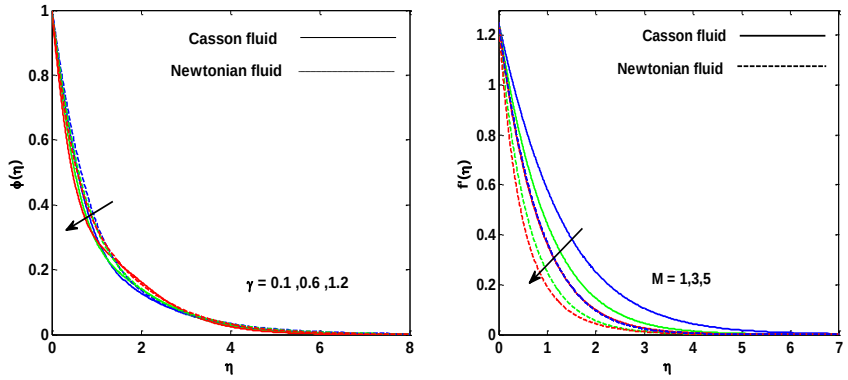

(a) Concentration profile for γ. **(b) Velocity profile for M.**

Fig. 11. Concentration and velocity profiles.

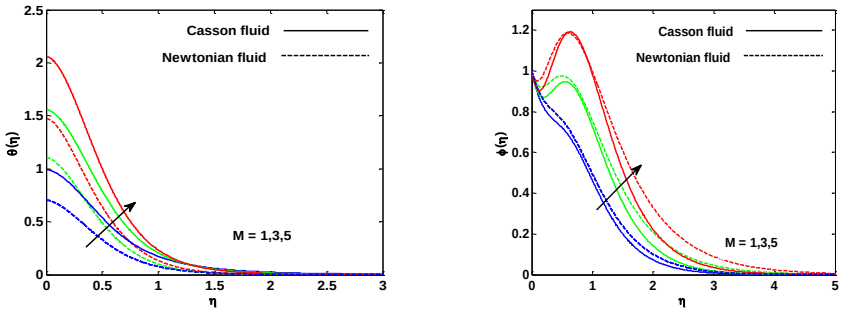

(a)Temperature profile for M. **(b)Concentration profile for M.**

Fig. 12. Temperature and concentration profiles.

The skin friction, the local Nusselt and local Sherwood number of both Casson nanofluid and Newtonian fluid are presented in Tables 2 and 3, respectively. It is observed that the skin-friction and Nusselt number decrease with the increase in the thermal Grashof number and solutal Grashof number, whereas, Sherwood number increases for both the fluids. With the increase in magnetic parameter the skin friction and Nusselt number increase, however, its reverse effects have been observed in Sherwood number. In Newtonian and Casson nanofluids flow skin friction increases with an increase in Le, Pr and γ, however, its reverse effects have been noticed in case of Nb, Nt, Ec and Bi. Here, Nusselt number increases with increase in Nb, Ec, Pr, Bi and γ and the reverse is the case for Nt and Nb. However, it is further revealed that the Sherwood number increases with an increase in Nt, Nb, Ec, Pr and γ and it decreases with an increase in Nb and Bi.

Table 2.Variations ofC_f, Nur and $Shr$for Cassonnanofluid.

M	Gr	Gc	Nb	Nt	Le	Ec	Pr	Bi	γ	*Cf*	*Nur*	*Shr*
1										2.4071	0.4645	1.2036
3										3.4711	0.4946	1.2073
5										4.3096	0.4957	1.2308
	.1									2.8623	0.4907	1.1945
	.6									2.4071	0.4645	1.2036
	1									2.0163	0.4603	1.1988
		.1								2.5621	0.4746	1.1998
		2								1.8391	0.4587	1.1982
		5								0.7471	0.4517	1.1986
			.1							2.4071	0.4645	1.2036
			.3							2.3687	0.4647	1.1561
			.6							2.2853	0.4648	1.1486
				.1						2.4071	0.4647	1.2036
				.3						2.3287	0.4706	1.3643
				.6						2.2549	0.4706	1.5545
					.5					2.3063	0.4776	0.4954
					1					2.3565	0.4763	0.7913
					2					2.4071	0.4645	1.2036
						.3				2.6530	0.4577	1.1122
						.5				2.5223	0.4615	1.1587
						.7				2.4071	0.4645	1.2036
							.5			2.4071	0.4645	1.2036
							.9			2.4213	0.4748	1.2565
							2			2.4226	0.4893	1.3061
								.1		2.4071	0.4645	1.2036
								.6		2.2943	0.9137	1.1407
								.9		2.1809	1.3693	1.0802
									.1	1.8473	0.4630	1.0558
									.6	2.5506	0.4663	1.2405
									1	3.4426	0.4795	1.4658

Table 3. Variation of C_f, Nur and Shr for Newtonian fluid.

M	Gr	Gc	Nb	Nt	Le	Ec	Pr	Bi	γ	*Cf*	*Nur*	*Shr*
1										1.3532	0.1547	0.9913
3										2.0100	0.1600	1.0077
5										2.5233	0.1605	1.0517
	.1									1.5928	0.1572	1.0172
	.6									1.3532	0.1547	1.0517
	1									1.1542	0.1539	1.0741
		.1								1.4745	0.1555	1.0445
		2								0.9050	0.1522	1.0830
		5								0.0375	0.1502	1.1393
			.1							1.3532	0.1547	1.0517
			.3							1.3259	0.1547	1.0523
			.6							1.2719	0.1547	1.0610
				.1						1.3532	0.1547	1.0517
				.3						1.3203	0.1545	1.1071
				.6						1.3023	0.1544	1.1571
					.5					1.3532	0.1567	1.0517
					1					1.3286	0.1547	0.6641
					2					1.3532	0.1546	1.0517
						.3				1.4575	0.1524	0.9857
						.5				1.4020	0.1554	1.0181
						.7				1.3532	0.1573	1.0517
							.5			1.3532	0.1547	1.0517
							.9			1.3677	0.1580	1.0767
							1			1.3713	0.1613	1.0996
								.3		1.3532	0.1547	1.0517
								.6		1.2652	0.3065	0.9934
								.9		1.1783	0.4560	0.9397
									.1	1.0186	0.1527	0.9405
									.6	1.4389	0.1553	1.0829
									1	1.9708	0.1597	1.2611

4. Conclusions

In this study, we considered the Brownian motion and thermophoresis effects on a non-linearly stretching sheet with Casson nanofluid in the presence of a magnetic field. There is a great focus and emphasis on the heat and mass transfer for the steady laminar Casson nanofluid with velocity slip and convective boundary condition. Using bvp4c of Matlab, the system of differential equations describing the model was solved. The main results of the present analysis are as follows:

- The temperature is enhanced for higher values of thermophoresis and Brownian motion parameter.
- Effects of thermophoresis and Brownian motion parameter on nanoparticle concentration are quite opposite than temperature.
- As the Prandtl number increases, the thermal boundary layer thickness decreases. The concentration profiles become steeper with an increase in the Lewis number.
- Larger thermal boundary layer thickness is produced with higher Brownian motion parameter.
- Spontaneous activity with smaller Eckert number brought together in terms of the energy equations describing the pressure changes, and body force in energy can be neglected.

Acknowledgement

We are very much thankful to the reviewers for their constructive suggestions to improve the quality of the manuscript.

Nomenclatures

a	Constant
B_i	Biot number
B_0	Magnetic field strength
C	Concentration
C_f	Local skin friction
C_P	Specific heat
C_w	Wall concentration
C_∞	Ambient concentration
D_B	Brownian motion parameter
D_T	Thermophoresis parameter
f	Velocity of fluid
g	Acceleration due to gravity
Gr	Thermal Grashofnumber
Gc	SolutalGrashofnumber
k	Thermal conductivity
Le	Lewis number
M	Magnetic parameter
Nt	Thermophoresis parameter
Nb	Brownian motion parameter
N_{ur}	Local nusseltnumber
Pr	Prandtl number
P_y	Yield stress of fluid
q_m	Mass flux
q_W	Heat flux
Sh_r	Local Sherwoodnumber
T	Temperature
T_w	Wall temperature
T_∞	Ambient temperature

Greek Symbols

α	Thermal diffusivity
β	Casson fluid parameter
β_T	Temperature expansion coefficient
β_c	Concentration expansion coefficient
γ	Velocity slip parameter
γ_0	Slip parameter
η	Similarity variable
θ	Dimensionless temperature.
μ_B	Plastic dynamic viscosity
ν	Kinematic viscosity
π_c	Critical value based on non-Newtonian
σ	Electrical conductivity
φ	Dimensionless concentration

References

1. Abolbashari, M.H.; Freidoonimehr, N.; Nazari, F.; and Rashid, M.M. (2015). Analytical modeling of entropy generation for Casson nano-fluid flow induced by a stretching surface. *Advanced Powder Technology*, 26(2), 542-552.
2. Hussain, T.; Shehzad, S.A.; Alsaedi, A.; Hayat, T.; and Ramzan, M. (2015). Flow of Casson nanofluid with viscous dissipation and convective conditions: A mathematical model. *Journal of Central South University*, 22(3), 1132-1140.
3. Rashid, M.M.; Abelman, S.; and Meher, N.F. (2013). Entropy generation in steady MHD flow due to a rotating porous disk in a nanofluid. *International Journal of Heat and Mass Transfer*, 62, 515-525.
4. Ramzan, M.; and Bilal, M. (2016). Three-dimensional flow of an elastico-viscous nanofluid with chemical reaction and magnetic field effects. *Journal of Molecular Liquids*, 215, 212-220.
5. Malvandi, A.; Moshizi, S.A.; Soltani, E.G.; and Ganji, D.D. (2014). Modified Buongiorno'smodel for fully developed mixed convection flow of nanofluids in a vertical annular pipe. *Computers & Fluids*, 89, 124-132.
6. Sreedevi, G.; Rao, R.R.; Chamkha, A.J.; and Prasada Rao, D.R.V. (2015). Mixed convective heat and mass transfer flow of nanofluids in concentric annulus. *Procedia Engineering*,127, 1048-1055.
7. Sheikholeslami, M.; Gorji-Bandpy, M.; Ganji, D.D.; Soleimani, S.; and Seyyedi, S.M. (2012), Natural convection of nanofluids in an enclosure between a circular and a sinusoidal cylinder in the presence of magnetic field. *International Communications in Heat and Mass Transfer*, 39(9), 1435-1443.
8. Mahanta, G.; and Shaw, S. (2015). 3D Casson fluid flow past a porous linearly stretching sheet with the convective boundary condition. *Alexandria Engineering Journal*, 54(3), 653-659.
9. Rahimi-Gorji, M.; Pourmehran, O.; Gorji-Bandpy, M.; and Gorji, T. B. (2015) CFD simulation of airflow behaviour and particle transport and deposition in different breathing conditions through the realistic model of human airways. *Journal of Molecular Liquids*, 209, 121-133.
10. Rahimi-Gorji, M.; Pourmehran, O.; Gorji-Bandpy, M.; and Ganji, D.D. (2016).Unsteady squeezing nanofluid simulation and investigation of its effect on important heat transfer parameters in presence of magnetic field. *Journal of the Taiwan Institute of Chemical Engineers*, 67, 467-475.
11. Rahimi-Gorji, M.; Gorji, T.B.; and Gorji-Bandpy, M. (2016). Details of regional particle deposition and airflow structures in a realistic model of human tracheobronchial airways: Two-phase flow simulation. *Computers in Biology and Medicine*,74 , 1-17.
12. Jafari, S.S.; and Freidoonimehr, N. (2015). Second law of thermodynamics analysis of hydromagnetic nano-fluid slip flow over a stretching permeable surface. *Journal of the Brazilian Society of Mechanical Sciences and Engineering*, 37(4), 1245-1256.
13. Wang, C.Y. (2002). Flow due to a stretching boundary with partial slip- an exact solution of the Navier-stokes equations. *Chemical Engineering Science*, 57(17), 3745-3747.
14. Sahoo, B. (2009). Effects of partial slip,viscous dissipation and joule heating on Vonkaman flow and heat transfer of an electrically conducting non-

Newtonian fluid. *Communications in Nonlinear Science and Numerical Simulation,*14(7), 2982-2998.

15. Salem, A.M.; and Fathy, R. (2012). Effects of variable properties on MHD heat and mass transfer flow near stagnation towards a stretching sheet in a porous medium with thermal radiation. *Chinese Physics B,* 21(5), 054701.
16. Fang, T.; and Zhang, J. (2009). Closed form exact solutions of MHD viscous flow over a shrinking sheet. *Communications in Nonlinear Science and Numerical Simulation,* 14(7), 2853-2857.
17. Das, M.; Mahto, R.; and Nandkeolyar, R. (2015). Newtonian heating effect on unsteady hydromagnetic Casson fluid flow past a flat plate with heat and mass transfer. *Alexandria Engineering Journal,* 54(4), 871-879.
18. Makinde, O.D.; and Aziz, A. (2010). MHD mixed convection from a vertical plate embedded in a porous medium with the convective boundary condition. *International Journal of Thermal Sciences,* 49(9), 1813-1820.
19. Aziz, A. (2009). Similarity solution for boundary layer over a plate with a convective surface boundary condition. *Communications in Nonlinear Science and Numerical Simulation,* 14(4), 1064-1068.
20. Hayat, T.; Shehzad, S.A.; Alsaedi, A.; and Alhothuali, M.S. (2012). Mixed convection stagnation point flow of Casson fluid with the convective boundary condition. *Chinese Physics Letters,* 29(11), 114704.
21. Shaw, S.; Kameswaran, P.K.; and Sibanda, P. (2013). Homogeneous-heterogenous reactions in micropolar fluid flow from a permeable stretching or shrinking sheet in porous medium. *Boundary Value Problems*, Article number: 77.
22. Shaw, S.; and Sibanda, P. (2013). Thermal instability in a non-Darcy porous medium saturated with nanofluid and with a convective boundary condition. *Boundary value problem*,1, 2013,186.
23. Rahimi-Gorji, M.; Ghajar,M.; Amir-Hasan, Kakaee.; and Ganji, D.D. (2017) Modeling of the air conditions effects on the power and fuel consumption of the SI engine using neural networks and regression. *Journal of the Brazilian Society of Mechanical Sciences and Engineering,* 39(2), 375-384.
24. Biglarian, M.; Rahimi-Gorji, M.; Pourmehran, O.; and Domairry, G. (2017). H_2O based different nanofluids with unsteady condition and an external magnetic field on permeable channel heat transfer. *International Journal of Hydrogen Energy,* 42(34), 22005-22014.
25. Michaelides, E.E. (2015). Brownian movement and thermophoresis of nanoparticles in liquids. *International Journal of Heat and Mass Transfer,* 81, 179-187.
26. Anbuchezhian, J.A.; Shrinivasan, K.; Chandrasekaran, K.; and Kandasamy, R. (2012). Thermophoresis and Brownian motion effects on boundary layer flow of nanofluid in presence of thermal stratification due to solar energy. *Applied Mathematics and Mechanics,* 33(6), 765-780.
27. Derjaguin, B.V.; and Yalamov, Y. (1965). Theory of thermophoresis of large of aerosol particles. *Journal of Colloid Science,* 20(6), 555-570.
28. Parola, A.; and Piazza, R. (2004). Particle thermophoresis in liquids. *The European Physical Journal E,* 15(3), 255-263.

29. Haddad, Z.; Abu-Nada, E.; Oztop, H.F.; and Mataoui, A. (2012). Natural convection in nanofluids are thermophoresis and Browinian motion effects significant in nanofluid heat transfer enhancement. *International Journal of Thermal Sciences*, 57, 152-162.

30. Falana, A.; Ojewale, O.A.; and Adeboje, T.B. (2016). Effect of Brownian motion and thermophoresis on a nonlinear stretching permeable sheet in a nanofluid. *Advances in Nanoparticles*, 5(1), 123-134.